^{96}_36Kr_60–Low-Z Boundary of the Island of Deformation at N =60

J. Dudouet, A. Lemasson, G. Duchêne, M. Rejmund, E. Clément, C. Michelagnoli, F. Didierjean, A. Korichi, G. Maquart, O. Stezowski, et al.

$^{96}_{36}Kr_{60}$–Low-Z Boundary of the Island of Deformation at $N = 60$

J. Dudouet,[1,*] A. Lemasson,[2] G. Duchêne,[3] M. Rejmund,[2] E. Clément,[2] C. Michelagnoli,[2] F. Didierjean,[3] A. Korichi,[4,2] G. Maquart,[1] O. Stezowski,[1] C. Lizarazo,[5,6] R. M. Pérez-Vidal,[7] C. Andreoiu,[8] G. de Angelis,[9] A. Astier,[4] C. Delafosse,[10] I. Deloncle,[4] Z. Dombradi,[11] G. de France,[2] A. Gadea,[7] A. Gottardo,[10] B. Jacquot,[2] P. Jones,[12] T. Konstantinopoulos,[4] I. Kuti,[11] F. Le Blanc,[3] S. M. Lenzi,[13,14] G. Li,[6] R. Lozeva,[3,4] B. Million,[15] D. R. Napoli,[9] A. Navin,[2] C. M. Petrache,[4] N. Pietralla,[5] D. Ralet,[5,4] M. Ramdhane,[16] N. Redon,[1] C. Schmitt,[2] D. Sohler,[11] D. Verney,[10] D. Barrientos,[17] B. Birkenbach,[18] I. Burrows,[19] L. Charles,[3] J. Collado,[20] D. M. Cullen,[21] P. Désesquelles,[4] C. Domingo Pardo,[7] V. González,[20] L. Harkness-Brennan,[22] H. Hess,[18] D. S. Judson,[22] M. Karolak,[23] W. Korten,[23] M. Labiche,[19] J. Ljungvall,[4] R. Menegazzo,[13] D. Mengoni,[13,14] A. Pullia,[15,24] F. Recchia,[13,14] P. Reiter,[18] M. D. Salsac,[23] E. Sanchis,[20] Ch. Theisen,[23] J. J. Valiente-Dobón,[9] and M. Zielińska[23]

[1]*Université, Université Lyon 1, CNRS/IN2P3, IPN-Lyon, F-69622 Villeurbanne, France*
[2]*GANIL, CEA/DRF-CNRS/IN2P3, BP 55027, 14076 Caen cedex 5, France*
[3]*Université de Strasbourg, CNRS, IPHC UMR 7178, F-67000 Strasbourg, France*
[4]*CSNSM, Université Paris-Sud, CNRS/IN2P3, Université Paris-Saclay, 91405 Orsay, France*
[5]*Institut für Kernphysik, Technische Universität Darmstadt, D-64289 Darmstadt, Germany*
[6]*GSI, Helmholtzzentrum für Schwerionenforschung GmbH, D-64291 Darmstadt, Germany*
[7]*Instituto de Física Corpuscular, CSIC-Universitat de València, E-46980 Valencia, Spain*
[8]*Department of Chemistry, Simon Fraser University, Burnaby, British Columbia V5A 1S6, Canada*
[9]*INFN, Laboratori Nazionali di Legnaro, Via Romea 4, I-35020 Legnaro, Italy*
[10]*Institut de Physique Nucléaire, IN2P3-CNRS, Université Paris Sud, Université Paris Saclay, 91406 Orsay Cedex, France*
[11]*Institute for Nuclear Research of the Hungarian Academy of Sciences, Pf. 51, H-4001 Debrecen, Hungary*
[12]*iThemba LABS, National Research Foundation, P.O. Box 722, Somerset West, 7129 South Africa*
[13]*INFN Sezione di Padova, I-35131 Padova, Italy*
[14]*Dipartimento di Fisica e Astronomia dell'Università di Padova, I-35131 Padova, Italy*
[15]*INFN, Sezione di Milano, Milano 20133, Italy*
[16]*LPSC, Université Grenoble-Alpes, CNRS/IN2P3, 38026 Grenoble Cedex, France*
[17]*CERN, CH-1211 Geneva 23, Switzerland*
[18]*Institut für Kernphysik, Universität zu Köln, Zülpicher Strasse 77, D-50937 Köln, Germany*
[19]*STFC Daresbury Laboratory, Daresbury, Warrington WA4 4AD, United Kingdom*
[20]*Departamento de Ingeniería Electrónica, Universitat de Valencia, 46100 Burjassot, Valencia, Spain*
[21]*Nuclear Physics Group, Schuster Laboratory, University of Manchester, Manchester M13 9PL, United Kingdom*
[22]*Oliver Lodge Laboratory, The University of Liverpool, Liverpool, L69 7ZE, United Kingdom*
[23]*IRFU, CEA/DRF, Centre CEA de Saclay, F-91191 Gif-sur-Yvette Cedex, France*
[24]*Dipartimento di Fisica, Università di Milano, I-20133 Milano, Italy*

(Received 27 January 2017; published 17 April 2017)

Prompt γ-ray spectroscopy of the neutron-rich ^{96}Kr, produced in transfer- and fusion-induced fission reactions, has been performed using the combination of the Advanced Gamma Tracking Array and the VAMOS + + spectrometer. A second excited state, assigned to $J^{\pi} = 4^{+}$, is observed for the first time, and a previously reported level energy of the first 2^{+} excited state is confirmed. The measured energy ratio $R_{4/2} = E(4^{+})/E(2^{+}) = 2.12(1)$ indicates that this nucleus does not show a well-developed collectivity contrary to that seen in heavier $N = 60$ isotones. This new measurement highlights an abrupt transition of the degree of collectivity as a function of the proton number at $Z = 36$, of similar amplitude to that observed at $N = 60$ at higher Z values. A possible reason for this abrupt transition could be related to the insufficient proton excitations in the $g_{9/2}$, $d_{5/2}$, and $s_{1/2}$ orbitals to generate strong quadrupole correlations or to the coexistence of competing different shapes. An unexpected continuous decrease of $R_{4/2}$ as a

function of the neutron number up to $N = 60$ is also evidenced. This measurement establishes the Kr isotopic chain as the low-Z boundary of the island of deformation for $N = 60$ isotones. A comparison with available theoretical predictions using different beyond mean-field approaches shows that these models fail to reproduce the abrupt transitions at $N = 60$ and $Z = 36$.

DOI: 10.1103/PhysRevLett.118.162501

The systematic evolution and the sudden changes of the properties of a many-body quantum system probe the basic interactions between its constituents. In the atomic nucleus, features such as shell closures and their migration [1–3], the onset of collectivity [4], shape coexistence [5–7], or the rapid transitions among them [8], result from the interplay between the mean field and correlations between individual nucleons [9]. The study of the evolution of these phenomena is crucial to understand the various facets of the nuclear force [2].

In the region of nuclei with $A \sim 100$ and $N \geq 60$, properties associated with large collective behavior were reported [10]. In this mass region, it is well established experimentally that Sr, Zr, and Mo isotopes exhibit a large prolate deformation in the ground state [11–13]. Contrarily, at the $N = 50$ shell closure, nuclei exhibit a structure typical of the single-particle motion in a spherical potential. The transition, between the spherical and well-deformed nuclei, appears to be abrupt at $N = 60$ [14–17]. This is associated with a shape-coexistence phenomenon where the coexisting spherical and deformed configurations suddenly invert at $N = 60$ [18–20]. This could be compared, on one hand, to the "island of inversion" associated with a rapid onset of collectivity observed at $N = 40$ near ^{64}Cr [21] and, on the other hand, to the smooth crossing of coexisting configurations in the neutron-deficient isotopes of Kr [22]. The low-Z boundary of this island of deformation has attracted much attention in the last years. In Ref. [23], ^{96}Kr was suggested to be at the critical point of the shape-phase transition near $A = 100$. Recent predictions from Monte Carlo Shell-Model (MCSM) calculations support the hypothesis of a quantum phase transition in Zr isotopes [18], and a recent measurement places ^{97}Rb ($Z = 37$) as the cornerstone of this island of deformation [24]. Both the transition to large collectivity at $N = 60$ in Sr-Mo and its sudden disappearance in Kr deserve further investigations [23,25].

Intense experimental efforts have been devoted to investigate the ^{96}Kr neutron-rich nucleus. Charge radii [26] and mass [23] measurements indicate a smooth development of collectivity in the isotopic chain of Kr. Mărginean *et al.* [27] reported a first excited state at 241 keV in ^{96}Kr, suggesting a well-developed deformation. This measurement was contradicted by Albers *et al.* [25,28], using Coulomb excitation, reporting a first 2^+ excited state at 554 keV and a correspondingly $B(E2; 2_1^+ \rightarrow 0_1^+)$ value much lower than those of ^{98}Sr and ^{100}Zr [see Fig. 1(a)]. Several theoretical approaches attempted to describe the structure of Kr isotopes. An oblate shape was proposed for ^{96}Kr, and the possibility of prolate-oblate shape coexistence was argued [28–31]. However, the sharp transitions at $N = 60$ and between Kr and Sr are not well reproduced simultaneously by those theories as well as the excited states beyond the first 2^+ state, highlighting that the underlying mechanisms remain to be understood.

To understand, quantify, and characterize the evolution of the nuclear structure along isotopic chains, a systematic study of the energies of the first excited states [$E(2^+)$ and $E(4^+)$], their ratio [$R_{4/2} = E(4^+)/E(2^+)$] and the corresponding reduced transition probabilities [$B(E2)$] are often used as primary indicators [4]. Figure 1(a) shows the corresponding experimental information available for isotopic chains of even-even nuclei with $50 \leq N \leq 64$ and $36 \leq Z \leq 42$ [32–34]. In general, a clear correlation between $R_{4/2}$ and $B(E2; 2_1^+ \rightarrow 0_1^+)/A$ is observed. In Mo,

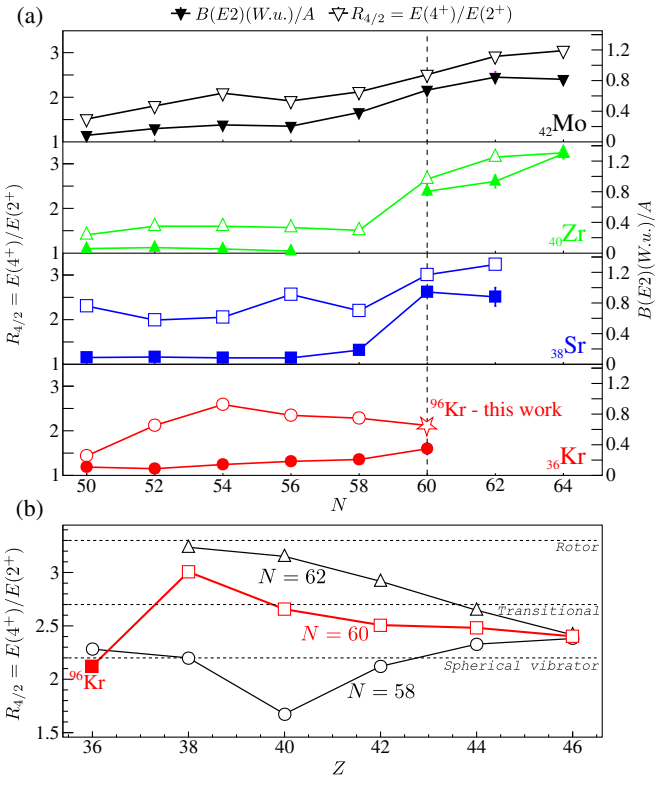

FIG. 1. (a) The ratio $R_{4/2} = E(4^+)/E(2^+)$ (open symbols, left axis) of the energies of the first excited 4^+ and 2^+ states and reduced transition probabilities expressed in Weisskopf units (solid symbols, right axis) in even-even nuclei as a function of the neutron number (N) [32–34]. (b) The $R_{4/2}$ ratio against the proton number Z for $N = 58$–62 isotonic chains. Horizontal dashed lines represent a schematic classification between spherical vibrational and rotor nuclei from Ref. [4].

the smooth increase of $R_{4/2}$ as a function of the neutron number illustrates the evolution from spherical (∼1.5) to well-deformed (∼3) nuclear shapes. Similarly, the corresponding $B(E2;2_1^+ \to 0_1^+)/A$ continuously increases, indicating a larger collectivity. For Sr and Zr, the trend is relatively flat for $N \leq 58$, while a sudden increase is observed at $N = 60$, and both indicators remain well correlated. In contrast, for Kr, $R_{4/2}$ increases more steeply than $B(E2;2_1^+ \to 0_1^+)/A$ for $N \leq 54$ and decreases beyond $N = 54$, while $B(E2;2_1^+ \to 0_1^+)/A$ continues increasing gradually. This is in contradiction with expectation, as the corresponding $E(2^+)$ and the $B(E2;2_1^+ \to 0_1^+)$ are well correlated in ^{96}Kr [25]. The aim of this work is to investigate whether this singular behavior of the $R_{4/2}$ trend persists at $N = 60$ in the neutron-rich ^{96}Kr. In this Letter, we report on a new measurement of 2^+ and 4^+ excited states in the neutron-rich nucleus ^{96}Kr populated in transfer- and fusion-induced fission processes.

The measurement was performed at GANIL using a ^{238}U beam at 6.2 MeV/u, with an intensity of 1 pnA, impinging on a 10-micron-thick ^{9}Be target. The advantage of the inverse kinematics used in this work is that fission fragments are forward focused at high velocities, resulting in both efficient detection and isotopic identification in the spectrometer. A single magnetic field setting of the large-acceptance spectrometer with its improved detection system VAMOS++ [35], possessing a momentum acceptance of around ±20%, was used to identify uniquely the fission fragments [36]. The spectrometer was placed at 28° with respect to the beam axis so as to optimize the acceptance for light fission fragments. The detection system at the focal plane of the spectrometer was composed of a multiwire parallel plane avalanche counter (MWPPAC), two drift chambers (x, y), and segmented ionization chambers (ΔE and E). The time of flight (TOF) was obtained using the signals from the two MWPPACs, one located after the target [37] and the other one at the focal plane (flight path ∼7.5 m). The parameters measured at the focal plane [(x, y), ΔE, E, and TOF] along with the known magnetic field were used to determine, on an event-by-event basis, the mass number (A), charge state (q), atomic number (Z), and velocity vector ($\vec{v}$) after the reaction for the detected fragments [35]. The prompt γ rays were measured in coincidence with the isotopically identified fragments, using the Advanced Gamma Tracking Array (AGATA) γ-ray tracking detector array [38] consisting of eight triple clusters placed in a compact configuration (13.3 cm from the target). The combination of the pulse-shape analysis [39,40] and the Orsay Forward Tracking (OFT) γ-ray tracking algorithm [41] allowed us to obtain the position of the first γ-ray interaction point. A Doppler correction was applied, using the precise determinations of the $\vec{v}$ obtained from VAMOS++ [37] and the γ-ray detection angle in AGATA, to calculate the γ-ray energy in the rest frame of the emitting fragment. A γ-ray energy resolution of 5 keV (FWHM) was obtained at 1.2 MeV (for recoiling fragments with v/c ranging between 0.095 and 0.135 and recoil angles varying by ∼20°).

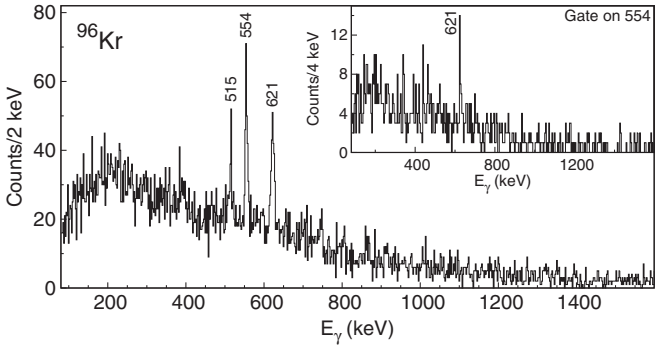

FIG. 2. Tracked γ-ray spectrum measured in coincidence with the isotopically identified fission fragment ^{96}Kr. (Inset) Tracked γ-ray spectrum measured in coincidence with the 554 keV transition.

Figure 2 shows the prompt γ-ray spectrum measured in coincidence with the ^{96}Kr ions detected in VAMOS++. Three transitions at 554(1), 621(2), and 515(2) keV can be seen in the spectrum. The 554 keV transition confirms the excitation energy of the 2_1^+ state of Ref. [25]. The 621 keV transition was observed in coincidence with the 554 keV transition (see the inset in Fig. 2). Its relative intensity is 90(25)% as compared to the 554 keV transition. It is interpreted as the transition depopulating the 4_1^+ excited state at 1175(3) keV. This assignment is supported by the systematic analysis of level energies and relative intensities of the neighboring nuclei and isotopic chains populated in fission under the similar experimental conditions and measured in the present experiment. The relative intensity of the 515 keV is 35(15)% as compared to the 554 keV transition. Because of the limited statistics, it was not possible to obtain a significant coincidence analysis for the 515 keV transition which was not placed in the level scheme. The nonobservation of this transition in the Coulomb excitation experiment [25] excludes that this transition depopulates the 2_1^+ state. Figure 3(a) shows the systematics of available experimental data for 2_1^+, 4_1^+, 3_1^-, and 2_2^+ as a function of the neutron number for Kr isotopes. The new level observed in this work follows the systematic trend. The present assignment as 4_1^+ of the newly observed level at 1175 keV results in $R_{4/2} = E(4^+)/E(2^+) = 2.12(1)$. The presence of low-lying 2_2^+ excited states in the Kr isotopic chain suggests the possible assignment of the 515 keV γ ray to the $2_2^+ \to 2_1^+$ transition.

The newly obtained $R_{4/2}$ ratio reported in the present work shows that $R_{4/2}$ continuously decreases till $N = 60$ as shown in Fig. 1(a). This extends the unexpectedly opposite trends of $R_{4/2}$ and $B(E2;2_1^+ \to 0_1^+)$ for the Kr

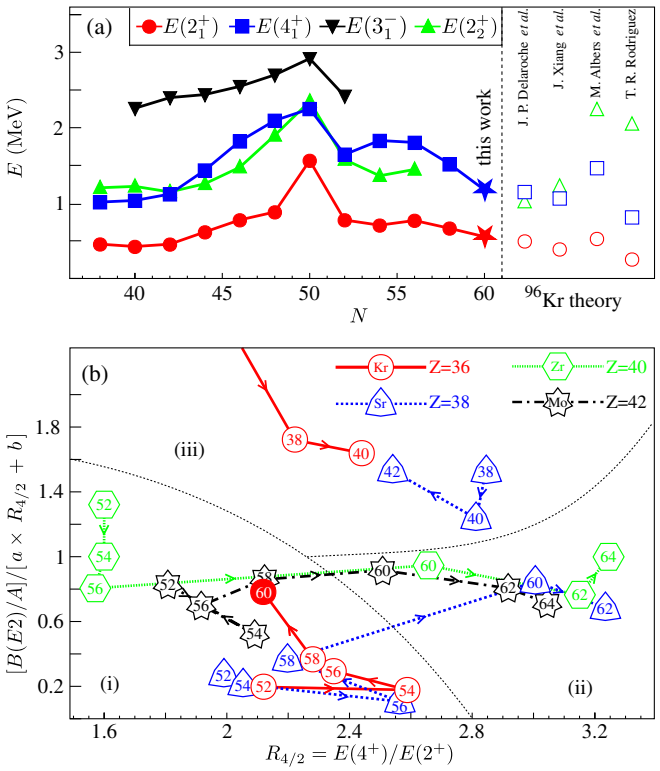

FIG. 3. (a) Systematic evolution of 2_1^+, 4_1^+, 3_1^-, and 2_2^+ states for the Kr isotopic chain. On the right-hand side are reported the latest theoretical mean-field calculations for the ^{96}Kr nucleus [28–31]. (b) Measured $[B(E2)/A]/[a \times R_{4/2} + b]$ values against $R_{4/2}$ with $B(E2)$ expressed in Weisskopf units, for isotopes of Mo, Zr, Sr, and Kr (where $a = 0.756$ and $b = -1.156$) [32–34]. Regions: (i) spherical vibrator, (ii) rotor, and (iii) prolate-oblate shape coexistence with strong mixing are also indicated. ^{72}Kr is out of scale at coordinates (1.86,2.89). The neutron number is indicated inside the symbols.

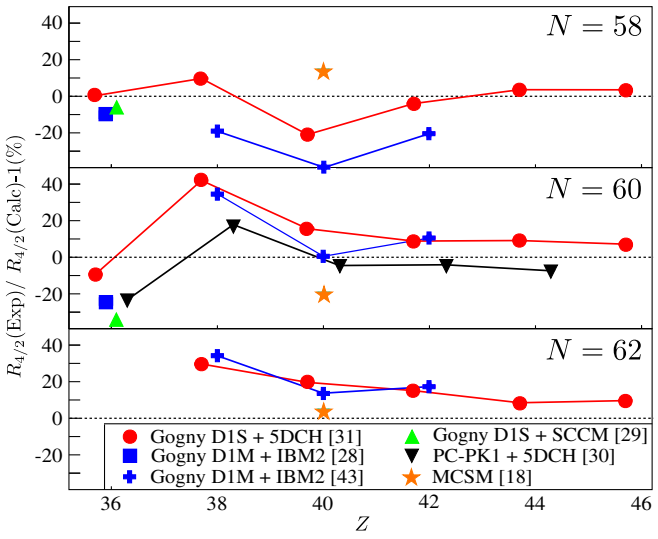

FIG. 4. Deviation between calculated and experimental $R_{4/2}$ ratios against the proton number for $N = 58$–62 isotonic chains and several theoretical predictions from the beyond mean-field approach (Gogny D1S + 5DCH [31], Gogny D1M + IBM2 [28,43], Gogny D1S + SCCM [29], and PC-PK1 + 5DCH [30]) and the MCSM [18].

neutron-rich isotopes and confirms the nonobservation of a sudden onset of collectivity at $N = 60$ as shown in Fig. 1(b). This figure represents the evolution of the $R_{4/2}$ ratio as a function of the proton number for isotones between $N = 58$ and $N = 62$ and shows the sharp transition between Sr and Kr at $N = 60$. Another way to investigate the correlation between the above observables is to study their ratio [i.e., $\sim B(E2; 2_1^+ \to 0_1^+)/R_{4/2}$] as a function of $R_{4/2}$. Figure 3(b) shows the correlation of $[B(E2)/A]/[a \times R_{4/2} + b]$ as a function of $R_{4/2}$ [where $B(E2)$ is expressed in Weisskopf units and a and b satisfy $B(E2)/A = [a \times R_{4/2} + b]$ for ^{94}Zr and ^{104}Zr]. This representation is similar to that introduced by Casten and Zamfir [42]. Three regions were classified according to the structural properties of the nuclei: (i) spherical vibrator, (ii) rotor, and (iii) prolate-oblate shape coexistence with strong mixing [42]. ^{96}Kr lies in the region of spherical vibrators. The lines connect the isotopes, and the arrows indicate the increasing neutron number. In the region of spherical vibrators, the characteristic feature of the $R_{4/2}$ ratio shows an absence of a clear trend. In contrast, in the region of rotors, a clear correlation emerges. However, for Kr isotopes, a regular trend starting from ^{90}Kr can be observed that does not head towards the rotor region, in contrast with other isotopic chains.

The neutron-rich Kr isotopes appear therefore to exhibit a different behavior than neighboring isotopic chains. To understand these differences from a theoretical point of view, it is necessary to reproduce the sudden transition observed for Sr, Zr, and Mo at $N = 60$, the very abrupt transition observed at $Z = 36$, and the relation between $R_{4/2}$ and $B(E2)$. Different theoretical approaches performed for the ^{96}Kr nucleus are available in the literature [25,29–31]. The right panel in Fig. 3(a) presents the calculated energies, using different beyond mean-field approaches, for the 2_1^+, 4_1^+, and 2_2^+ levels in ^{96}Kr. For this nucleus, Delaroche *et al.* [31] show the best agreement with the experimental data. Figure 4 shows the deviation of the calculated $R_{4/2}$ ratio (in percent) from various theoretical works for the isotonic chains $N = 58$, 60, and 62 as a function of the proton number [18,28–31,43]. Positive values refer to theoretically underestimated $R_{4/2}$ and could be interpreted as an insufficient degree of collectivity, while negative values indicate a too-strong degree of collectivity. Only Ref. [31] provides theoretical predictions for all the nuclei in this region. Most of the predictions were obtained from beyond mean-field calculations using the Gogny D1S/D1M [28,29,31,43] or PC-PK1 [30] energy density functional and different beyond mean-field mapping procedures. It can be seen from Fig. 4 that theoretical predictions of beyond mean-field calculations from Refs. [30,31,43] have a similar trend but fail to reproduce the abrupt transition at $N = 60$ and between

$Z = 36$ and $Z = 38$. For $N \geq 60$, the degree of collectivity is largely insufficient while approaching $Z = 38$, though it tends to be reasonably large for $Z > 40$. Results from Refs. [28,29], obtained also from beyond mean-field approaches, show a larger disagreement, where available. The continuous decrease of the $R_{4/2}$ [see Fig. 1(a)] ratio in Kr beyond $N = 54$ remains puzzling and could be related to a shape-coexistence phenomenon. Beyond mean-field calculations consistently predict [28,29,31] an oblate ground-state band in ^{96}Kr and also a second 0^+ state at an excitation energy between 1.0 and 1.5 MeV with a prolate character. Rodriguez [29] also suggests a rapid shape change along the first excited band in ^{94,96}Kr. Similar behavior was reported for the neutron-deficient ^{72}Kr isotope, where a shape change occurs along the ground-state band at a low spin, resulting in a reduced $R_{4/2}$ value [44].

Recently, a microscopic description of the shape coexistence in the Zr isotopic chain using the MCSM approach was reported [18,20], which reproduces quite well the experimental data. These calculations provide for the first time a microscopic description of the quantum shape-phase transition in Zr isotopes at $N = 60$. Figure 4 shows that these predictions are in very good agreement with the experimental data for $N = 62$, while they display a different trend than the mean-field results for $N = 58$, 60. The MCSM calculations, performed in a very large model space, describe the ground state of ^{98}Zr as spherical, while the deformed low-lying 0_2^+ state is predicted as a multiparticle-multihole excitation of protons from the fp shell to the intruder $g_{9/2}$ and $d_{5/2}$ orbitals and neutrons into the $g_{7/2}$ and intruder $h_{11/2}$ orbitals. The two 0^+ states cross in excitation energy in ^{100}Zr, having a deformed ground state. The development of a deformation in this mass region is explained in Ref. [18] as resulting from the change in the shell structure induced by the monopole central and tensor components of the proton-neutron interaction for specific particle-hole excitations. As a consequence, intruder orbits are lowered, thus favoring the cross-shell excitations. The combination of the monopole and the quadrupole components of the nuclear interaction results in the development of a deformation in Zr isotopes. It will be crucial to pursue theoretical efforts, within the microscopical framework of MCSM calculations, to understand the sudden transition at $Z = 36$ as well as the unexpected trend of $R_{4/2}$, highlighted in this work.

Similar phenomena have been observed in other regions of neutron-rich nuclei, the so-called islands of inversion, and can be understood in terms of the dynamical symmetries pseudo- and quasi-SU3 that apply in shell-model spaces that include the relevant degrees of freedom for the development of quadrupole collectivity [45,46]. In this mass region, the relevant valence space for protons consists of the $1f_{5/2}$, $2p_{3/2}$, $2p_{1/2}$, $1g_{9/2}$, $0g_{7/2}$, $2d_{5/2}$, $3s_{1/2}$ orbitals, while the neutrons move in the space spanned by $2d_{5/2}$, $2d_{3/2}$, $3s_{1/2}$, $1g_{7/2}$, $1h_{11/2}$, $2f_{7/2}$, $3p_{3/2}$. The development of a deformation in this valence space requires a critical number of protons and neutrons. An analogy between the $Z = 40$, $N \sim 60$ region and the island of inversion at $Z \sim 24$, $N = 40$ [21] could be drawn. The onset of a deformation develops at $N = 38$ in Cr ($Z = 24$) and at $N = 40$ in Fe ($Z = 26$) isotopes. Isotones with $N = 36$ remain transitional, as it is for ^{96}Kr with $Z = 36$ in the $Z = 40$, $N \sim 60$ deformation region. This similarity highlights possible analog microscopic mechanisms where an insufficient proton occupation of the quasi-SU3 orbits ($g_{9/2}$, $d_{5/2}$, $s_{1/2}$) prevents the development of strong quadrupole correlations in Kr at $N = 60$.

In summary, the present work establishes for the first time the second excited $J^\pi = 4^+$ state in the neutron-rich ^{96}Kr. The deduced ratio $R_{4/2} = 2.12(1)$ confirms that Kr represents the low-Z edge of the island of deformation at $N = 60$. Its unexpectedly low value is in contradiction with the previously established smooth development of collectivity along the Kr isotopic chain. The value of $R_{4/2}$ and the rapid onset of deformation in the region are not reproduced by available beyond mean-field theoretical models. Recent advances of Monte Carlo Shell-Model calculations in this region should allow a progression in understanding the microscopic nuclear structure of ^{96}Kr and the moderate development of collectivity in this isotope compared to heavier $N = 60$ isotones. Further experimental investigations in even more neutron-rich Kr isotopes shall reveal if the decreasing $R_{4/2}$ trend does persist. In parallel to multistep Coulomb excitation and spectroscopy of higher excited states, direct reactions using neutron-rich radioactive ion beams will allow us to probe the orbital occupation of relevant states in this mass region.

We acknowledge the important technical contributions of J. Goupil, G. Fremont, L. Ménager, J. Ropert, C. Spitaels, and the GANIL accelerator staff. We acknowledge S. Péru-Desenfants for fruitful discussions. This work was supported by the Bundesministerium für Bildung und Forschung under No. 05P09RDFN4 and No. 05P12RDFN8 and by the Helmholtz International Center for Facility for Antiproton and Ion Research. D. R. was partially supported by the P2IO Excellence Laboratory. D. S. acknowledges support by the European Union and the State of Hungary, co-financed by the European Regional Development Fund under Project No. GINOP-2.3.3-15-2016-00034. A. G. and R. P. were partially supported by Ministerio de Economía y Competitividad and Generalitat Valenciana, Spain, under Grants No. FPA2014-57196-C5 and No. PROMETEOII/2014/019 and by the European Union FEDER funds. The authors also acknowledge support from the European Union Seventh Framework Programme through ENSAR, Contract No. 262010.

*Corresponding author.
j.dudouet@ipnl.in2p3.fr

[1] T. Otsuka, R. Fujimoto, Y. Utsuno, B. A. Brown, M. Honma, and T. Mizusaki, Phys. Rev. Lett. **87**, 082502 (2001).
[2] O. Sorlin and M. G. Porquet, Prog. Part. Nucl. Phys. **61**, 602 (2008).
[3] T. Otsuka, T. Suzuki, M. Honma, Y. Utsuno, N. Tsunoda, K. Tsukiyama, and M. Hjorth-Jensen, Phys. Rev. Lett. **104**, 012501 (2010).
[4] R. F. Casten, *Nuclear Structure from a Simple Perspective* (Oxford University, New York, 2001).
[5] K. Heyde and J. Wood, Rev. Mod. Phys. **83**, 1467 (2011).
[6] F. Nowacki, A. Poves, E. Caurier, and B. Bounthong, Phys. Rev. Lett. **117**, 272501 (2016).
[7] T. Otsuka and Y. Tsunoda, J. Phys. G **43**, 024009 (2016).
[8] R. F. Casten, Nat. Phys. **2**, 811 (2006).
[9] E. Caurier, G. Martínez-Pinedo, F. Nowacki, A. Poves, and A. P. Zuker, Rev. Mod. Phys. **77**, 427 (2005).
[10] J. Hamilton, in *Treatise Heavy Ion Science* (Plenum Press, New York, 1989), Vol. 8, Chap. 1, pp. 2–98.
[11] E. Cheifetz, R. C. Jared, S. G. Thompson, and J. B. Wilhelmy, Phys. Rev. Lett. **25**, 38 (1970).
[12] F.K. Wohn, J. C. Hill, R. F. Petry, H. Dejbakhsh, Z. Berant, and R. L. Gill, Phys. Rev. Lett. **51**, 873 (1983).
[13] W. Urban *et al.*, Eur. Phys. J. A **22**, 241 (2004).
[14] P. Campbell, I. Moore, and M. Pearson, Prog. Part. Nucl. Phys. **86**, 127 (2016).
[15] B. Cheal *et al.*, Phys. Lett. B **645**, 133 (2007).
[16] F. Charlwood *et al.*, Phys. Lett. B **674**, 23 (2009).
[17] B. Cheal *et al.*, Phys. Rev. Lett. **102**, 222501 (2009).
[18] T. Togashi, Y. Tsunoda, T. Otsuka, and N. Shimizu, Phys. Rev. Lett. **117**, 172502 (2016).
[19] E. Clément *et al.*, Phys. Rev. Lett. **116**, 022701 (2016).
[20] C. Kremer *et al.*, Phys. Rev. Lett. **117**, 172503 (2016).
[21] S. M. Lenzi, F. Nowacki, A. Poves, and K. Sieja, Phys. Rev. C **82**, 054301 (2010).
[22] E. Clément *et al.*, Phys. Rev. C **75**, 054313 (2007).
[23] S. Naimi *et al.*, Phys. Rev. Lett. **105**, 032502 (2010).
[24] C. Sotty *et al.*, Phys. Rev. Lett. **115**, 172501 (2015).
[25] M. Albers *et al.*, Phys. Rev. Lett. **108**, 062701 (2012).
[26] M. Keim, E. Arnold, W. Borchers, U. Georg, A. Klein, R. Neugart, L. Vermeeren, R. E. Silverans, and P. Lievens, Nucl. Phys. **A586**, 219 (1995).
[27] N. Mărginean *et al.*, Phys. Rev. C **80**, 021301 (2009).
[28] M. Albers *et al.*, Nucl. Phys. **A899**, 1 (2013).
[29] T. R. Rodriguez, Phys. Rev. C **90**, 034306 (2014).
[30] J. Xiang, J. M. Yao, Y. Fu, Z. H. Wang, Z. P. Li, and W. H. Long, Phys. Rev. C **93**, 054324 (2016).
[31] J.-P. Delaroche, M. Girod, J. Libert, H. Goutte, S. Hilaire, S. Péru, N. Pillet, and G. F. Bertsch, Phys. Rev. C **81**, 014303 (2010).
[32] http://www.nndc.bnl.gov/ensdf/.
[33] T. Rzaca-Urban *et al.*, Eur. Phys. J. A **9**, 165 (2000).
[34] K. Li *et al.*, Int. J. Mod. Phys. E **20**, 1825 (2011).
[35] M. Rejmund *et al.*, Nucl. Instrum. Methods Phys. Res., Sect. A **646**, 184 (2011).
[36] A. Navin and M. Rejmund, in *McGraw-Hill Yearbook of Science and Technology* (McGraw-Hill, New York, 2014), p. 137.
[37] M. Vandebrouck, A. Lemasson, M. Rejmund, G. Fremont, J. Pancin, A. Navin, C. Michelagnoli, J. Goupil, C. Spitaels, and B. Jacquot, Nucl. Instrum. Methods Phys. Res., Sect. A **812**, 112 (2016).
[38] S. Akkoyun *et al.*, Nucl. Instrum. Methods Phys. Res., Sect. A **668**, 26 (2012); E. Clément *et al.*, Nucl. Instrum. Methods Phys. Res., Sect. A **855**, 1 (2017); A. Gadea *et al.*, Nucl. Instrum. Methods Phys. Res., Sect. A **654**, 88 (2011).
[39] R. Venturelli and D. Bazzacco, LNL annual Report No. 2004, http://www.micros2005.lnl.infn.it/~annrep/read_ar/2004/contrib_2004/pdfs/FAA122.pdf.
[40] B. Bruyneel, B. Birkenbach, and P. Reiter, Eur. Phys. J. A **52**, 70 (2016).
[41] A. Lopez-Martens, K. Hauschild, A. Korichi, J. Roccaz, and J.-P. Thibaud, Nucl. Instrum. Methods Phys. Res., Sect. A **533**, 454 (2004).
[42] R. F. Casten and N. V. Zamfir, Phys. Rev. Lett. **70**, 402 (1993).
[43] K. Nomura, R. Rodríguez-Guzmán, and L. M. Robledo, Phys. Rev. C **94**, 044314 (2016).
[44] H. Iwasaki *et al.*, Phys. Rev. Lett. **112**, 142502 (2014).
[45] A. P. Zuker, J. Retamosa, A. Poves, and E. Caurier, Phys. Rev. C **52**, R1741 (1995).
[46] A. P. Zuker, A. Poves, F. Nowacki, and S. M. Lenzi, Phys. Rev. C **92**, 024320 (2015).